Lawrence W. Fritz
Dr. Hellmut H. Schmid
NOAA, National Ocean Survey
Rockville, Maryland 20852

Stellar Calibration of the Orbigon Lens

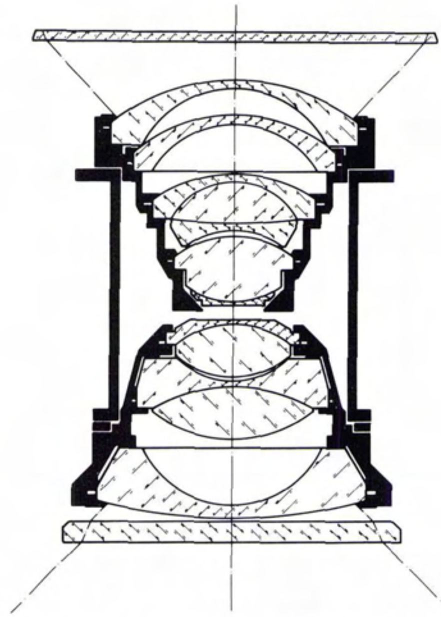

Fig. 1. Schematic cross section of the Orbigon. (Courtesy of Wild Heerbrugg Ltd.)

This 80-mm, 90°-angle lens was to have been used for precision measurements on the Apollo 17 mission that has been cancelled.

Introduction

Since 1965 *NASA* has supported the concept of establishing a lunar geodetic reference system. The system is based primarily on the determination of the geometry of the moon surface from overlapping metric photographs in combination with simultaneously executed stellar attitude photographs, laser altimeter measurements, and the determination of the sequence of all of these measurements with respect to Universal Time. The need for a high-precision photogrammetric camera to acquire the overlapping terrain photographs was recognized as an essential component of the overall sensor package. Because of mission constraints, a camera with a format of 114 × 114 mm had to be considered. Thus, to provide the wide-angle characteristics necessary for assuring the geometric strength of the photogrammetric triangulation, a maximum focal length of 80 mm became mandatory. Particularly because of the desire to eliminate, for metric precision, the need for image-motion compensation (a rather serious problem because of the high velocity of the space vehicle with respect to the moon's surface), it was necessary to consider a lens with as large a geometric aperture as possible to effect short time exposures. Under these circumstances it is most important that the lens system be characterized by a favorable *T*-stop performance.

On the other hand, these two requirements were in no way to impair the lens resolution, because of the anticipated small-scale photographs (about 1 part in a million or more) that would result from the space vehicle's height of approximately 100 km above the surface of the moon.

No lens that could fulfill these requirements was in existence. Therefore, Dr. Bertele of the Wild Heerbrugg Ltd. of Switzerland was approached with the problem of developing such a lens. This development was to be based on experience in the design of high-performance wide-angle systems currently used in precision photogrammetry. For the development of a metric camera, a reimbursable contract with NASA was initiated in 1970 with Wild Heerbrugg Ltd. as subcontractor. The prototype lens cone featured an unacceptable nonplanar, raised border of the focal plane reseau and, according to information given by the Wild factory, included an unstable glass for some of the lens components. After these defects were corrected, the final lens cone was delivered to the National Geodetic Survey in 1972.

This "Orbigon" lens (shown in Figure 1) has the following nominal characteristics:

Angle of view over the diagonal	90°
Focal length	80.2 mm
Maximum aperture	1:3.5
Corresponding maximum *T*-stop	1:6.8
Resolution at 1:3.5 on 500 lines/mm test plates for high contrast targets AWAR	133 lines/mm
Focal plane reseau square pattern of reseau distances	10 mm

observation pier permanently set in the ground is enclosed by a small building. The roof of the building may be moved to provide a wide-angle (90°) field of view of the sky.

Figure 2 shows the operational setup used to obtain stellar exposures with the Orbigon lens cone. A two-inch thick, circular, glass optical flat was placed on the steel-plate upper surface of the observation pier. For each exposure a ¼ inch thick, Kodak 103-F spectroscopic emulsion microflat photographic plate was placed directly on the optical flat. Then the glass focal plane (reseau plate) of the Orbigon cone was placed directly on the photographic plate. The wooden guide shown in Figure 2 was used to center the photographic plate and the cone onto the optical flat, as all of the setup was performed in total darkness. A remotely controlled and separately supported capping shutter was centered over the lens cone. This arrangement prevents

ABSTRACT: *A complete evaluation has been made of a new lens cone designed for photogrammetric surveys taken from orbital spacecraft. The f/3.5 wide-angle Wild Orbigon lens contains a reseau and is color corrected. A comprehensive stellar calibration of the lens at three apertures was performed at NOS. A unique economical technique for combining multiple plates in a combined adjustment is presented. The combined adjustment from multiple plate exposures contained 24,454 degrees of freedom. The adjustment results show that over the entire cone format the transformed radial symmetric distortion does not exceed 4.1 ± 0.06 μm and the lens decentering distortion does not exceed 3.0 ± 0.08 μm. Results of lens resolution and light transmission tests performed at NBS indicate an AWAR of 133 lines/mm at full aperture and a maximum variation of focal plane illumination of 12 percent.*

An extensive geometrical and optical performance calibration of the lens cone was performed by the National Ocean Survey and the National Bureau of Standards; the results of these calibrations are presented here. Because of the termination of the Lunar Apollo Program with Apollo Mission 17, there was, unfortunately, no opportunity to incorporate the lens in the flight package. The purpose of this presentation of detailed performance data is to acquaint the photogrammetric community with the existence of this lens system, which under the overall size constraints, is believed to constitute an optimum photogrammetric sensor.

FIELD PROCEDURE

All stellar exposures were obtained at the NOS calibration test site located in Beltsville, Maryland. At the site, a concrete and steel

any vibrations generated by the operation of the shutter from affecting the cone-plate setup during an exposure. Thermistor probes were taped to the pier, to the optical flat, and to the focal-plane edge of the cone to monitor temperature during exposure. The exposures were not begun until the temperatures of all three probes were consistent and stable. During exposure, probe temperatures were recorded every 15 minutes to provide data for the removal of any systematic image shifts in the event of changes in temperature. A dark cloth shroud (not shown) encircled the set-up to prevent exposure from stray light.

Preliminary tests demonstrated that whenever the aperture was not wide open (f/3.5) starlight did not provide sufficient luminance to expose adequately the focal-plane reseau crosses. Therefore, a flat board was painted with a 3M Velvet Coating that provides a

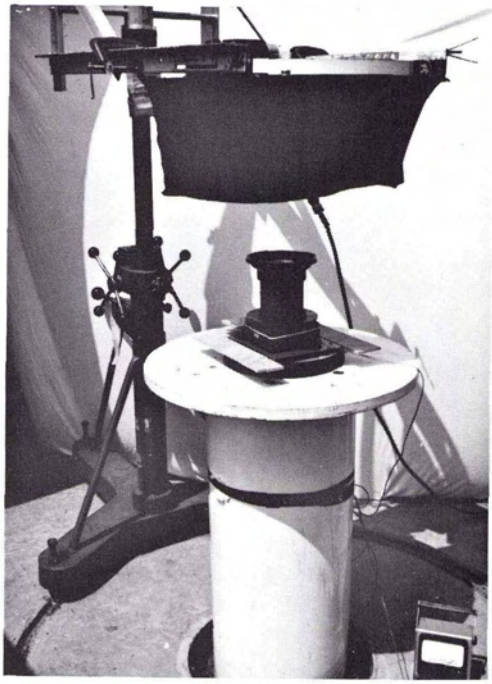

FIG. 2. Orbigon lens cone calibration setup.

near perfect diffusing surface. At the conclusion of the $f/4$ and $f/5.6$ exposures the diffuser board was suspended horizontally above the cone setup. Then the board was evenly illuminated by artificial light for a predetermined time. This post-illumination provided ideal exposure of the reseau crosses without deteriorating the stellar imagery.

The stellar exposures were scheduled for cloud-free, moonless nights. The total time required for each exposure was approximately two and one-half hours. Operation of the capping shutter was controlled by a paper-tape-fed programmer unit interfaced with a precise timing unit. Greenwich Mean Time and all capping shutter commands and responses were recorded on 30-channel electric

TABLE 1. DUTY CYCLE OF CAPPING SHUTTER

Open	*Close*	*Repetitions*
20 sec.	10 sec.	2, 3, 4, or 5
0.6 sec.	39.4 sec.	5
20 sec.	20 sec.	1
1.2 sec.	38.8 sec.	5
20 sec.	20 sec.	1
3.2 sec.	96.8 sec.	5
20 sec.	20 sec.	1
6.2 sec.	33.8 sec.	5
20 sec.	20 sec.	1
10 sec.	30 sec.	5

recording chart paper. The capping shutter program produced the duty cycle shown in Table 1.

A calibration-plate exposure requires four runs(or *trails*) of the duty cycle, each separated by a 7-to-10-minute break. This sequence provides a unique image and time identification code on the exposed plate. Each trail contains up to 25 measurable images for a single star.

Three primary aperture settings, $f/3.5$, $f/4$, and $f/5.6$, were chosen for the calibration. Two plate exposures were made at each aperture to minimize the effect of any atmospheric refraction anomalies, any possible large plate deformations, and to provide even and complete imagery throughout the cone format. Exposures were made with the cone pointed towards the zenith, with the cone for the second plate of each aperture rotated 180° from the first (denoted as North or South cone orientation).

MEASUREMENT AND DATA REDUCTION

The plate-measurement procedure involved the selection of cataloged stars of eighth magnitude or brighter and with a standard error of position of less than 0.4 seconds of arc. Each plate was measured twice, with the second set of measurements made with the plate rotated 180° on the comparator. The 11.4-cm square format of the Orbigon cone has 121 evenly-spaced reseau crosses. Five images from each of the four different star trails were chosen for measurement in each square centimeter of each plate. This selection made available for adjustment up to 2420 individual star images per plate. The selective spacing of the star imagery provides idealized geometry and statistical redundancy for minimizing the influence of any local plate deformations and photographic emulsion shifts.

Measurements of each plate were corrected for comparator errors and all double measurements were meaned. After computing an approximate camera orientation, the star-image measurements were transformed to right ascensions-declinations for Epoch 1950 and catalog identified. Next the identified star catalog coordinates were updated to their apparent position at the event epoch (Bush, 1973). The updated star catalog coordinates were then corrected for atmospheric refraction and diurnal aberration, and transformed to a local cartesian coordinate system. Then a simultaneous least-squares adjustment was computed using a single camera orientation mathematical model (Slama 1972). This mathematical model holds the camera position fixed $(X_0=Y_0=Z_0=O)$ and solves for the parameters that uniquely describe all recognized systematic departures from a central perspective. These departures may be summarized as those attributable to lens design, lens element manufacture, lens element assembly, and lens cone orientation with respect to the focal-plane reseau. The 11 camera calibration parameters of the mathematical model are identified and symbolized as follows:

Primary calibrated focal length	C
Principal point coordinates	x_P, y_P
Point of symmetry coordinates	x_S, y_S
Radial symmetric lens distortion model coefficients	K_1, K_2, K_3
Decentering lens distortion model coefficients	K_4, K_5
Orientation angle of axis of maximum tangential distortion	Φ_T

In addition to these parameters, the mathematical model contains a choice of one to three sets of exterior orientation angles $(\alpha_j, \omega_j, \kappa_j)$ and two deformation parameters. The deformation parameters allow for differential scalers (Cx, Cy) along the x and y plate-coordinate axes and an angle of nonorthogonality (ε) between them. These deformation parameters are included in the reduction of each stellar plate to allow for any linear scale errors in the comparator measurements, for any possible lack of perpendicularity of the ways of the comparator, and to absorb any differential variation in scale of the cone focal plane caused by thermal stresses.

A mathematical expression (Slama, 1972) which contains all of the mentioned parameters is

$$x_i^* = \left(\frac{C_x m}{q} + x_p\right)\left(1 + \frac{\Delta R}{d} + D_x\right) - x_s\left(\frac{\Delta R}{d} + D_x\right) - y_i\epsilon$$

$$y_i^* = \left(\frac{C_y n}{q} + y_p\right)\left(1 + \frac{\Delta R}{d} + D_y\right) - y_s\left(\frac{\Delta R}{d} + D_y\right)$$

where x_i°, y_i° are the measured image coordinates, and

$$\begin{bmatrix} m \\ n \\ q \end{bmatrix} = M \begin{bmatrix} X \\ Y \\ Z \end{bmatrix}.$$

Here M represents a rotation matrix of the exterior orientation parameters (α,ω,κ) and X,Y,Z are the updated star catalog coordinates transformed to a local cartesian coordinate system.

The radial symmetric distortion is expressed by

$$\Delta R = K_1 d^3 + K_2 d^5 + K_3 d^7$$

where d is the radial distance of the true image from the point of symmetry and determined by

$$d^2 = (x_i - x_s)^2 + (y_i - y_s)^2 = dx^2 + dy^2.$$

The decentered lens distortion is expressed by

$$D_x = (K_4 + K_5 d^2) \times \left(\frac{3\,dx^2 + dy^2}{dx} \cos\phi_t + 2dy \sin\phi_t\right)$$

$$D_y = (K_4 + K_5 d^2) \times \left(\frac{3dy^2 + dx^2}{dy} \sin\phi_t + 2dx \cos\phi_t\right).$$

Single-Plate Calibration Results

Table 2 contains a summary of the six individual plate reductions. In each adjustment the star positions from the FK-4 catalog were weighted using a standard error of position of 0.3 seconds of arc, whereas stars from other catalogs were weighted using a standard error of 0.4 seconds of arc. All positions given are based on an origin at the center cross of the reseau plate in a left-handed coordinate system as viewed on the focal plane.

Fifteen evenly distributed reseau crosses were measured on each negative plate. The reseau was calibrated at the Swiss Office of Weights and Measures at a temperature of 20.0°C. The mean measurement lab temperature at NOS is 22.0°C. To standardize the camera calibrations made at NOS and at Wild, a 20.0°C calibration temperature was adopted. Therefore, all NOS measurements were scaled by a factor of 0.9999838 based on a thermal

TABLE 2. SINGLE-PLATE CALIBRATIONS

Aperture	*f/3.5*		*f/4*		*f/5.6*	
Plate Number	*1320*	*2325*	*1424*	*2422*	*1523*	*2521*
Exposure Date	25 Mar. 72	12 May 72	12 May 72	9 Apr. 72	18 Apr. 72	9 Apr. 72
Cone Orientation	North	South	North	South	North	South
Exposure Temp (°C)	0.°0	11.7°	15.6°	0.6°	13.3°	2.8°
Scaler	.9998591	.9997863	.9997708	.9999257	.9997931	.9999002
Measurer	McClure	Rich	McClure	Lewis	Lewis	Rich
Pointing Precision	1.23	1.66	1.10	1.30	1.34	1.47
No. of Catalog Stars	228	188	217	242	199	154
No. of Unknown Stars	51	40	38	33	42	44
No. of Star Images	2223	2089	2191	2327	2285	2179
ε (sec arc)	−1.4	+6.3	−0.7	−4.3	+2.6	−4.3
Cx (μm)	80,175.49	80,175.42	80,169.02	80,170.43	80,171.61	80,171.43
Cy (μm)	80,175.26	80,176.10	80,171.74	80,170.16	80,170.57	80,170.75
x_P (μm)	−26.28	−18.39	−20.08	−19.18	−15.69	−19.70
y_P (μm)	−7.54	+1.92	−1.75	−4.09	+3.23	−8.14
x_S (μm)	+640.4	+1,960.3	+495.8	+653.5	−59.4	+1,606.2
y_S (μm)	−989.8	+1,143.9	+113.6	+543.0	−3,009.5	−455.4
K_1	+3.1602−1	+2,8423−1	+3.4158−1	+4,2606−1	+3.2730−1	+3.6121−1
K_2	−9.8841+1	−8.0781+1	−1.0271+2	−1.3591+2	−8.9978+1	−9.7877+1
K_3	+8.6655+3	+5.9101+3	+8.4257+3	+1.2787+4	+6.9584+3	+7.9470+3
K_4	+8.1706−4	+9.9064−4	+5.2302−4	+8.2068−4	−9.0853−5	+9.4516−4
K_5	+3.7180−2	−6.8632−2	+7.1291−2	+7.6589−3	+1.8162−1	−3.1152−2
Φ_T	−266°07′	259°39′	−287°27′	276°05′	−267°55′	−298°37′
m_P (μm)	2.90	2.51	2.84	2.78	2.73	2.65
m_0 (μm)	2.48	2.51	2.49	2.49	2.50	2.50

coefficient for photographic plates of 8.1 × 10^{-6} per degree C.

However, adjustment of the thus corrected negative reseau cross measurements with respect to the calibrated Wild cross positions for each plate revealed an average discrepancy in scale by a factor of 1.0001446 (negative too large), although the photographic emulsion and the cone reseau were in direct contact during exposure. Ensuing orthogonal measurements made of the reseau on a Wild STK1 comparator confirmed the scale of the Wild reseau values. A further investigation revealed that the reseau was projected during the photographic process into the spectroscopic 103-F emulsion. Assuming a 25-30 μm thick emulsion with an index of refraction of 1.65, it was found that the exposure of the average reseau cross produced an image centroid 21 μm deep into the emulsion. Therefore, to refer all measurements to the calibrated reseau, they were scaled accordingly before adjustment.

The pooled standard error of a single weighted observation of a single plate (m_P) from the six plates of Table 2 is 2.74 μm. The reduction of each plate *(i)* contained three sets *(j)* of exterior orientation parameters $(\alpha_{ij}, \omega_{ij}, \kappa_{ij})$. These three camera directions were carried in the adjustment to subdue any effects of camera or pier motion during the two and one-half hour exposures. The largest amount of camera motion detected was 3.5 seconds of arc (Plate #1523).

Multiple-Plate Calibration Results

A multiple-plate adjustment was performed to obtain single sets of camera calibration parameters for each aperture setting and a single set of calibration parameters most representative for all three aperture settings. Rather than combining all observations of each plate in a grand simultaneous least-squares solution, the following equivalent generalized weighted-mean adjustment was performed (Pope, 1969).

$$\bar{X} = \left\{\sum_{i=1}^{n}\left(\Sigma_{X_i}^{-1}\right)\right\}^{-1}\left\{\sum_{i=1}^{n}\left(\Sigma_{X_i}^{-1} X_i\right)\right\}$$

$$\Sigma_{\bar{X}} = m_0^2\left\{\sum_{i=1}^{n}\left(\Sigma_{X_i}^{-1}\right)\right\}$$

$$m_0^2 = \frac{\sum_{i=1}^{n}(\nu_i)}{\nu} + \frac{1}{\nu}\sum_{i=1}^{n}\{(X_i - \bar{X})^T \Sigma_{X_i}^{-1}(X_i - \bar{X})\}.$$

Here n is the total number of plates combined, $\bar{X}$ are the calibration parameters from the combined adjustment of n plates, X_i are the calibration parameters of plate i, Σ_{xi} is the variance-covariance matrix of the calibration parameters from the adjustment of plate i, $\Sigma\bar{X}$, is the variance-covariance matrix of the calibration parameters from the combined adjustment, m_o is the standard error of an observation of unit weight, ν_i is the number of degrees of freedom of the ith plate, and ν is the total number of degrees of freedom for the combined adjustment.

This generalized weighted mean adjustment produces results identical to a grand simultaneous least squares solution. In the adjustment, a single set of the eleven calibration parameters $(C, x_P, y_P, x_S, y_S, K_1\text{-}K_5, \Phi_T)$ common to all plates is computed. The adjustment permits the multiple exterior orientation parameters $(\alpha_{ij}, \omega_{ij}, \kappa_{ij})$ and the separate deformation parameters $(Cx_i, Cy_i, \varepsilon_i)$ of each plate to assume new values without solving for them explicitly. This arrangement is obviously well suited for economical computer usage.

Table 3 summarizes the results of the multiple plate adjustments for each of the three apertures calibrated. The last columns of Table 3 summarize the results of a three-aperature, six-plate generalized weighted mean adjustment that comprises a single set of calibration parameters most representative of all three apertures.

Diagnostic Plots of the Calibration

To analyze the results of the adjustments performed and to provide a full appreciation of the stellar calibration system, a series of graphic plots are generated as itemized in Table 4. Examples are presented in Figures 3 through 9.

Histograms are plotted from residuals, after meaning the double measurements of each plate, to determine whether any significant measurement biases are present. Other histograms are plotted from the residuals generated in the single camera calibration adjust-

TABLE 3. MULTIPLE-PLATE CALIBRATIONS

Aperture	*f/3.5*		*f/4*		*f/5.6*		*combined f/3.5,f/4,f/5.6*	
	Value	*Standard Error*	*Value*	*Standard Error*	*Value*	*Standard Error*	*Value*	*Standard Error*
C (μm)	80,174.86	.06	80,169.00	.06	80,169.97	.06	80,171.03	.04
x_P (μm)	−21.52	.06	−19.29	.06	−22.11	.05	−20.50	.03
y_P (μm)	−2.76	.08	−4.06	.07	4.60	.07	−.04	.04
x_S (μm)	−188.7	186.6	1,356.1	203.8	1,467.2	120.0	1,063.6	86.3
y_S (μm)	−2,127.6	369.5	−542.4	273.1	−1,162.6	328.1	−1,163.7	177.1
K_1	+3.0558−1	9.38−3	+4.1071−1	1.01−2	+3.6011−1	9.02−3	3.6494−1	5.49−3
K_2	−9.2105+1	3.57+0	−1.3083+2	3.84+0	−9.9918+1	3.26+0	−1.1011+2	2.04+0
K_3	+7.6095+3	4.05+2	+1.2057+4	4.41+2	+8.1283+3	3.53+2	+9.5244+3	2.27+2
K_4	+7.4688−4	8.68−5	+4.4638−4	8.01−5	+1.0948−3	8.13−5	+7.8152−4	4.44−5
K_5	+5.6488−2	1.47−2	+9.4269−2	1.24−2	−1.5387−3	1.33−2	+5.0665−2	7.46−3
Φ_T	−271°22′	2°40′	−279°31′	2°46′	−252°27′	2°15′	−271°12′	1°24′
m_o	1.09		1.18		1.20		1.22	
υ	7992		8390		8052		24454	
m_p (μm)	2.50		2.49		2.50		2.50	
m_{p^a} (μm)	2.61		2.71		2.74		2.75	

m_o = the standard error of an observation of unit weight (unitless scaling factor)
m_p = the mean standard error of an observation of unit weight of a plate before combined adjustment
m_{p^a} = the mean standard error of an observation of unit weight of a plate after combined adjustment

TABLE 4. CALIBRATION GRAPHICS

	Single Plate Solution	Multiplate Single Aperture Solution	Multiplate Multi-Aperture Solution
Histogram plot of residuals			
a. From Mean of Double Measurements			
(1)x coordinate	*		
(2)y coordinate	*		
(3)x and y coordinates	*		
b. From Single Camera Orientation			
(1)x coordinate	*		
(2)y coordinate	*		
(3)x and y coordinates	Fig. 3		
Plot of Star Images Measured	*	Fig. 5	
Single Camera Orientation Residual Plots			
a. Plate Residual Vector	Fig. 4		
b. Radial Component	Fig. 4		
c. Tangential Component	Fig. 4		
Plot of Systematic Lens Distortion			
a. Total Systematic Distortion	*	Fig. 6	Fig. 6
b. Radial Symmetric Distortion	*	Fig. 6	Fig. 6
c. Lens Decentering Distortion	*	Fig. 6	Fig. 6
Plot of Systematic Distortion Profiles			
a. Radial Symmetric Distortion	*	Fig. 7	Fig. 7
b. Lens Decentering Distortion	*	Fig. 9	Fig. 9
c. Transformed Radial Systematic Distortion	*	Fig. 8	Fig. 8

* Plotted but not shown in this report.

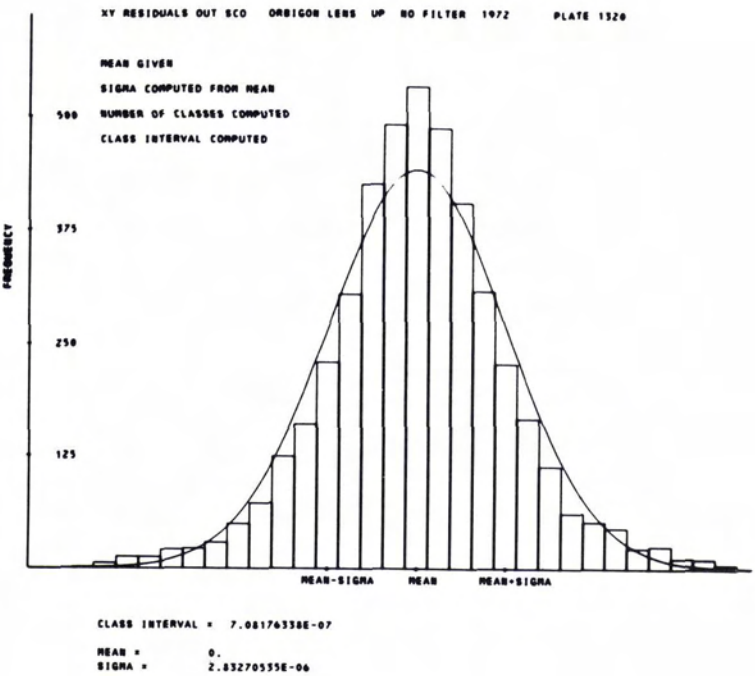

FIG. 3. A histogram of all residuals from the single camera calibration adjustment of Plate #1320.

ment of each plate to reveal if any unmodeled systematic errors are present in the data. The histograms are generated for each x and y coordinate residual and for combined x,y coordinate residuals. All of the histograms are superimposed on a plot of the Gaussian normal distribution curve. (See example, Figure 3.)

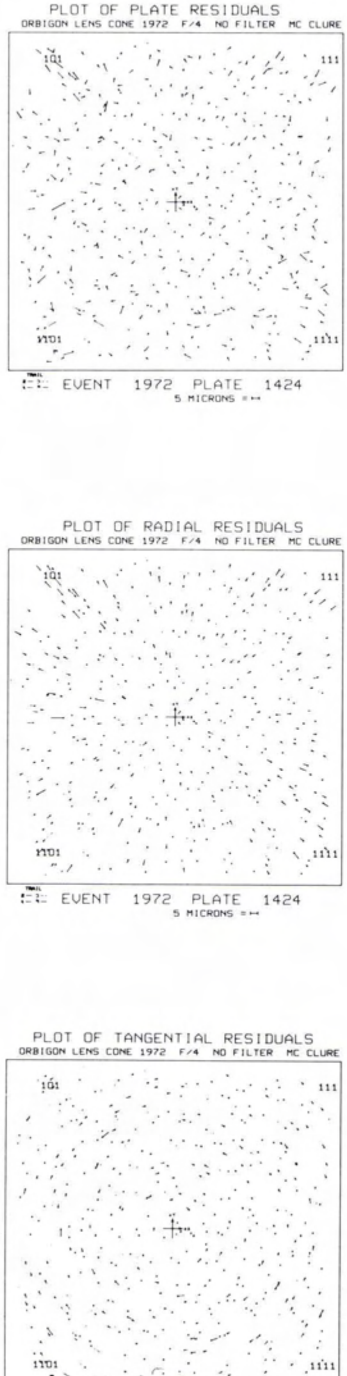

FIG. 4. Plot of residuals from camera calibration adjustment of plate #1424.

After each single plate adjustment, a series of four-color plots are produced that show the residuals from each of the four star trails in a different color. Figure 4 shows these plots (in black and white) for *f*/4 plate #1424. The plot of plate residuals shows the total residual vector, whereas the plots of radial residuals and tangential residuals contain the respective components of the total vector. Each vector plotted represents a subtrail of five images of a single star.

Another four-color plot is generated showing all star images used in the adjustment. A composite measured star image plot for the two plates exposed at *f*/3.5 is shown in Figure 5.

Figure 6 contains a series of systematic lens distortion characteristics. Plots are shown for each aperture and for the six-plate, three-aperture solution. The plot entitled "Math Model of Total Systematic Distortion" is a plot of the total systematic lens distortion model determined from the least-squares adjustment. The other two plots show each of the two components of the total systematic lens distortion model, i.e., the radial symmetric component and the lens decentering component. The dashed line represents the axis of maximum tangential distortion, defined by the angle Φ_T and drawn through the point of symmetry (x_S, y_S). All plots shown in Figures 4, 5, and 6 are keyed to the focal plane by the corner reseau numbers.

Figures 7-9 give the distortion profile curves for each of the three apertures and for the final six-plate, three-aperture solution. The first plot shows the Radial Symmetric Lens Distortion at the Primary Calibrated Focal Length. The plot in Figure 8 shows the same Radial Symmetric Lens Distortion transformed to a focal length where the positive and negative lobes of the enclosed areas beneath the curve are equal. The dashed lines on all three figures represent the one-sigma envelope of curve accuracy. Each of the distortion curves is plotted to its maximum extent of the exposure format.

ADDITION LENS EVALUATIONS

The Orbigon lens cone was sent to the National Bureau of Standards for resolution, light transmittance, and focal plane illumination tests. Table 5 contains the results of the resolving power tests on high-resolution (minimum of 500 lines/mm) photographic plates.

Table 6 contains the results of the axial transmission tests, including the *f*- and *T*-numbers for each aperture setting.

Four exposure plates were made to determine the light distribution across diagonals

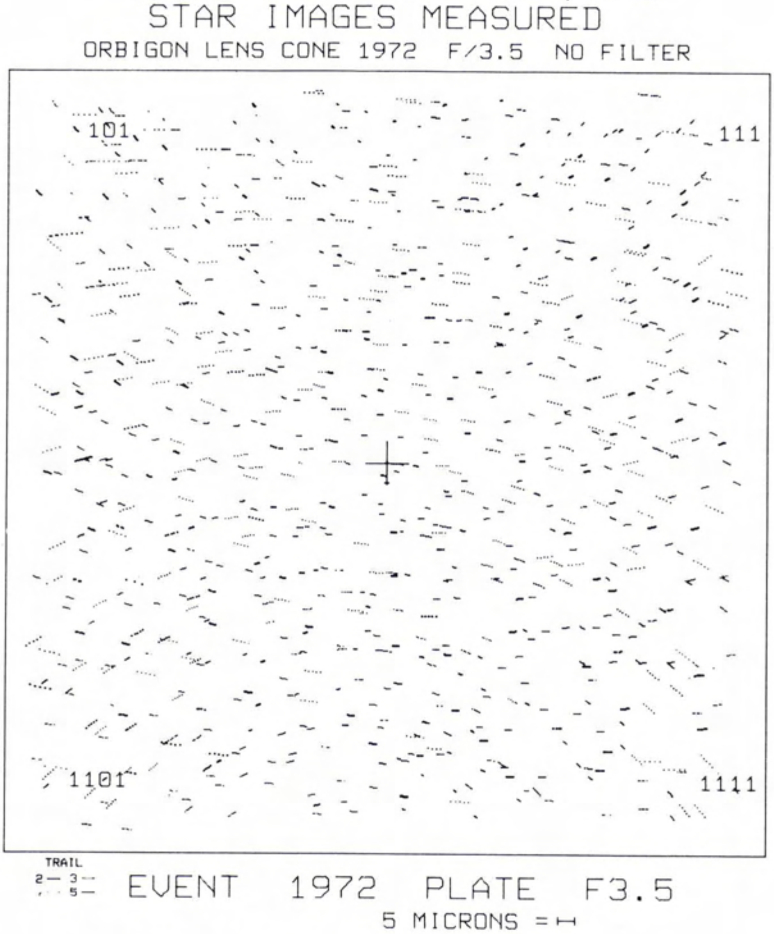

FIG. 5. All images measured on two plates at *f*/3.5.

TABLE 5. RESOLVING POWER

High Resolution Plates				*Field Angle*					
Aperture	*0°*	*5°*	*10°*	*15°*	*20°*	*25°*	*30°*	*35°*	*40°*
f/3.5							AWAR 133.0		
Tangential	181	161	161	128	128	128	114	114	51
Radial	181	161	181	256	161	161	161	181	29
f/4							AWAR 137.7		
Tangential	181	161	161	128	128	128	128	114	51
Radial	181	161	181	256	181	161	181	181	32
f/5.6							AWAR 141.9		
Tangential	181	161	161	128	128	144	128	114	51
Radial	181	161	203	256	203	181	181	181	32

TABLE 6. AXIAL TRANSMISSION

Aperture	*Transmittance on Axis*	*Geometric f-Number*	*T-Number*
f/3.5	26.3%	f/3.49	T/6.80
f/4	26.1%	f/3.90	T/7.64
f/5.6	27.1%	f/5.56	T/10.68
f/8	25.4%	f/7.84	T/15.57
f/11	26.9%	f/11.25	T/21.71
f/16	28.6%	f/15.99	T/29.92

of the focal plane format. Results of microdensitometer traces across the eight diagonals revealed an average variation in light distribution of 8 percent, with a maximum of 12 percent and a minimum of 5 percent.

References

Bush, Anna Mary (Geodetic Research and Development Laboratory, National Ocean Survey, NOAA, Rockville, Md.), "The Reduction of Photographic Plate Measurements for Satellite Triangulation," *NOAA Technical Report* NOS 60, June 1973, 154 pp.

Pope, Allen J. (Geodetic Research and Development Laboratory, National Ocean Survey, NOAA, Rockville, Md.), personal communication, 1969.

Slama, Chester C., "A Mathematical Model for the Simulation of a Photogrammetric Camera Using Stellar Control," *NOAA Technical Report* NOS 55, Geodetic Research and Development Laboratory, National Ocean Survey, National Oceanic and Atmospheric Administration, U.S. Dept. of Commerce, Rockville, Md., Dec. 1972, 138 pp.

(Figures 6-9 are on the next pages.)

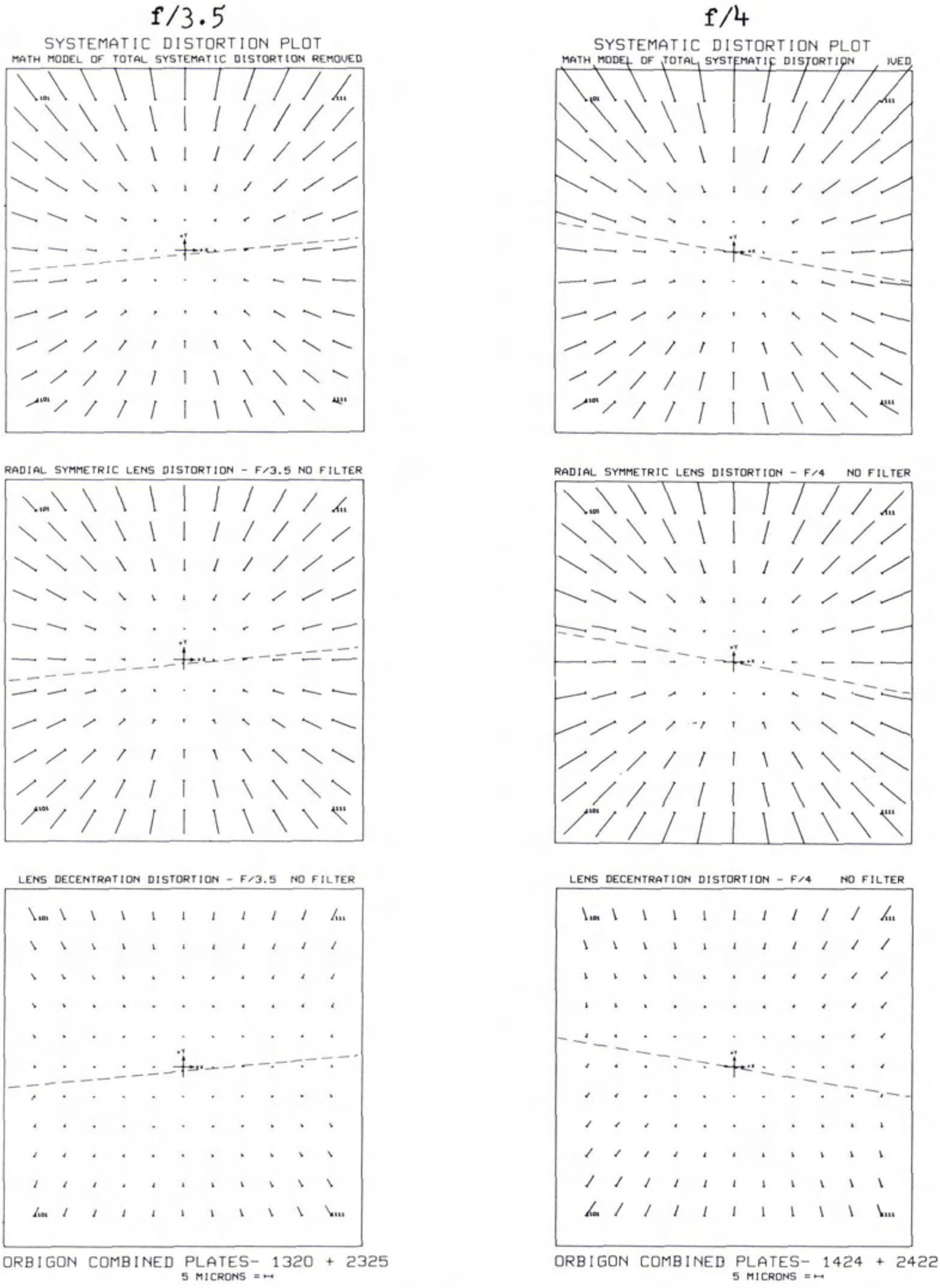

FIG. 6. Computed distortion model from calibrations of *f*/3.5, f/4, *f*/5.6 and combined apertures.

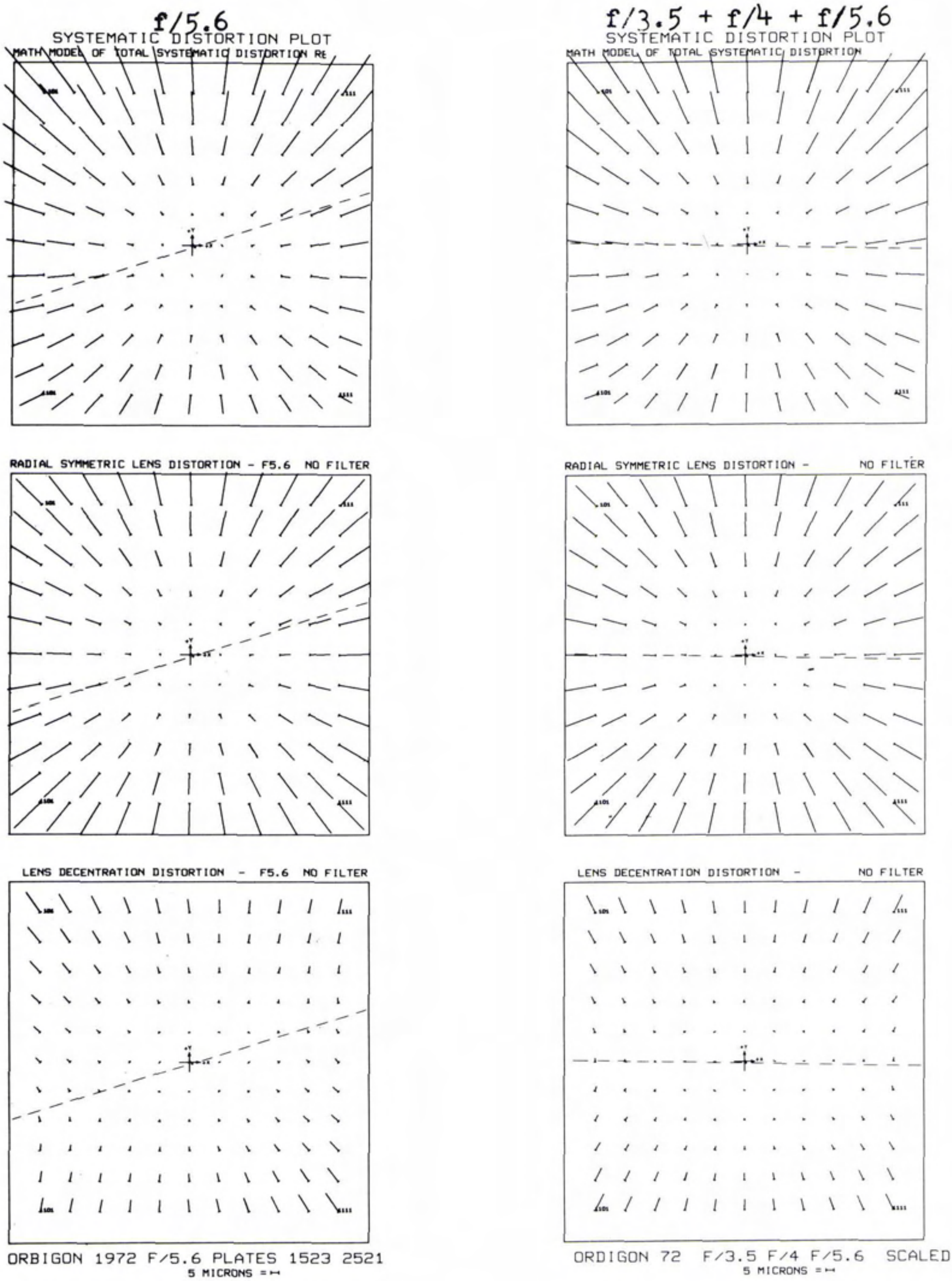

FIG. 6. (Continued)

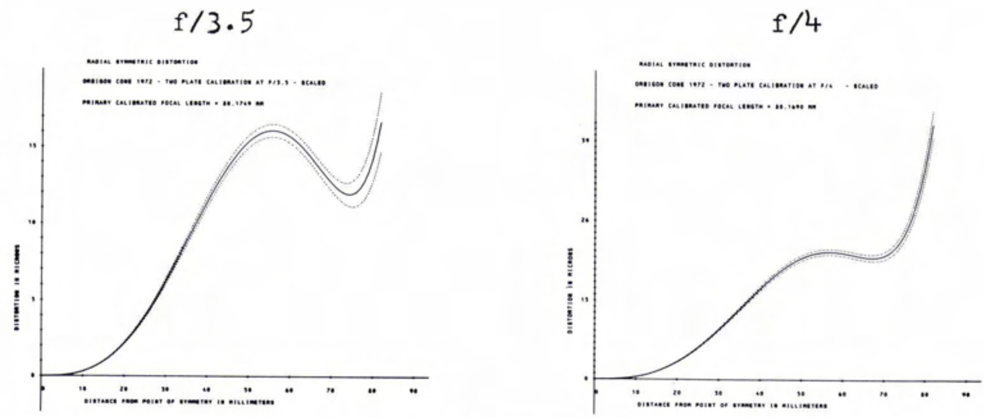

FIG. 7. Radial Symmetric Distortion.

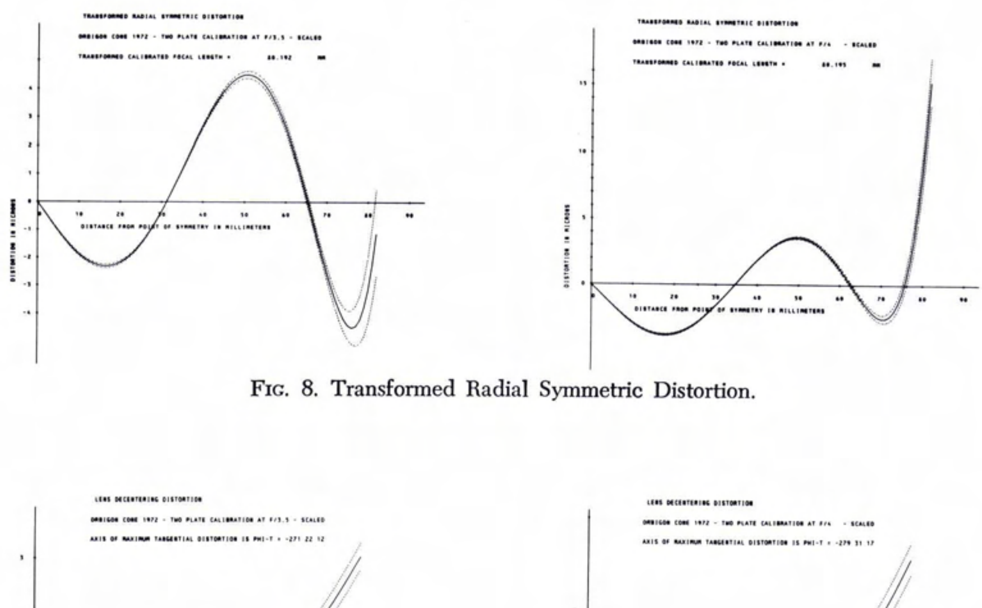

FIG. 8. Transformed Radial Symmetric Distortion.

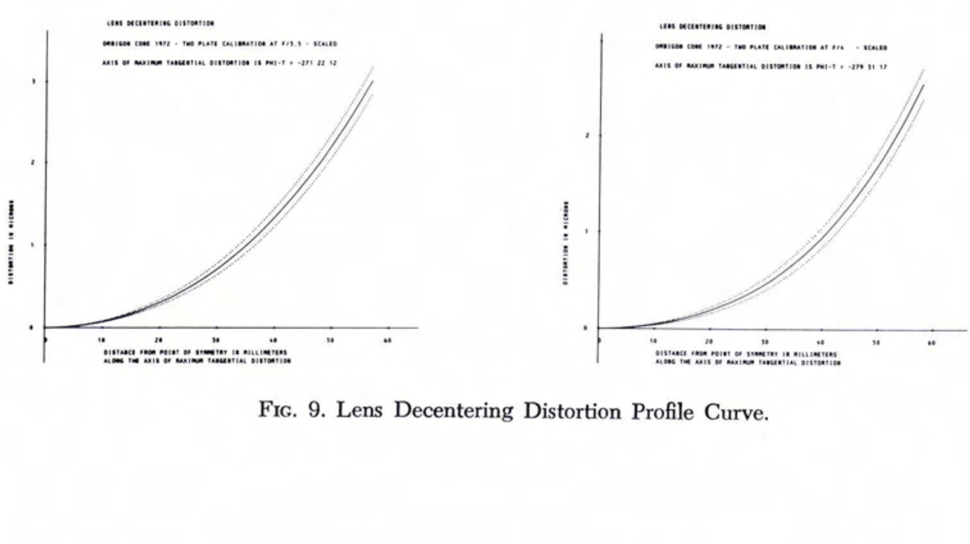

FIG. 9. Lens Decentering Distortion Profile Curve.

f/5.6 f/3.5 + f/4 + f/5.6

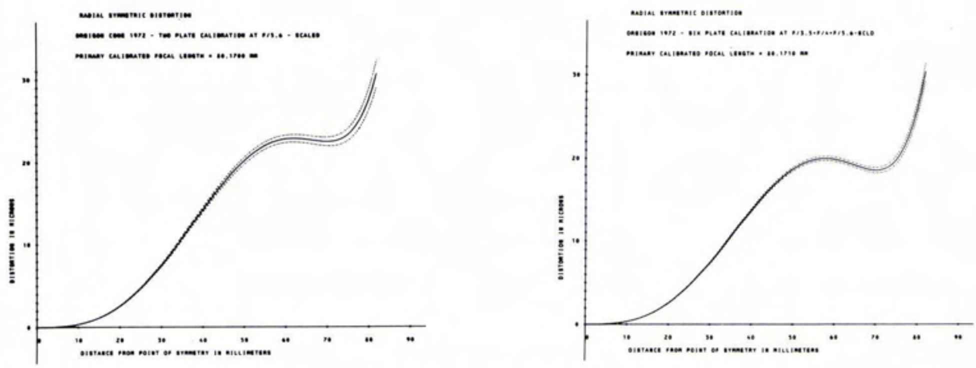

FIG. 7. (Continued)

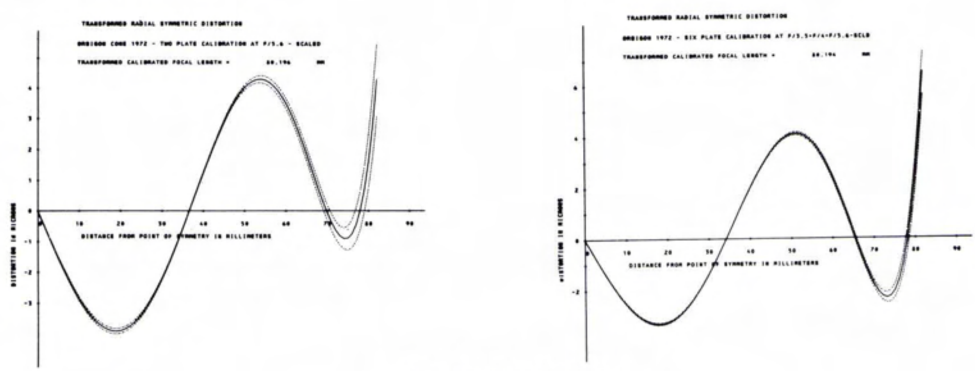

FIG. 8. (Continued)

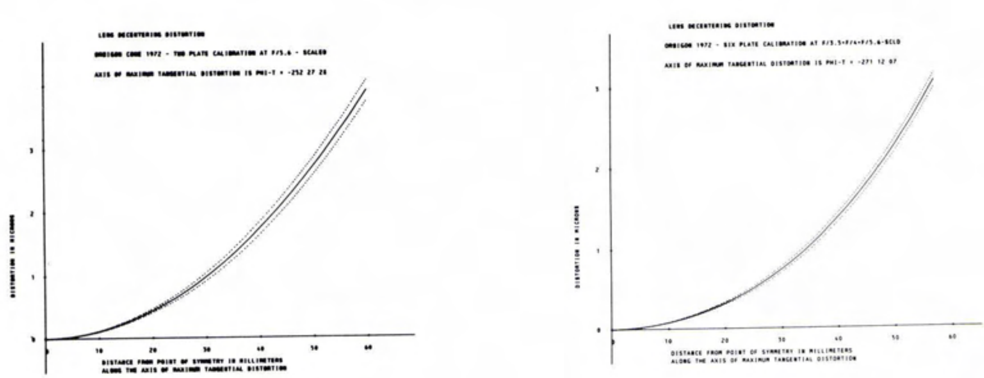

FIG. 9. (Continued)